INTELLIGENT TOOLS AND METHODS FOR RADIO SCIENCE

EMF Exposure Assessment in Spatial and Temporal Scale with Uncertainty Quantification

***Yukun Liu*[1], *Shanshan Wang*[1], *Paul Lagouanelle*[1], *Yarui Zhang* [2], *Joe Wiart*[1]**

[1] *Chaire C2M, LTCI, Télécom Paris, Institut Polytechnique de Paris, Palaiseau, France*
[2] *SATIE, ENS Paris-Saclay, CNRS, Université Paris-Saclay, Gif-sur-Yvette, France*

Keywords: Sensor Networks, Uncertainty Quantification, Spatial Temporal Prediction

Abstract

The deployment of 5G and beyond networks has heightened public concerns regarding radio frequency electromagnetic field (RF-EMF) exposure. Measurement based assessments are often affected by uncertainties arising from device noise, spatial environmental variability, and temporal fluctuations in base station (BS) activity. This paper presents a comprehensive framework on spatial and temporal prediction of RF-EMF exposure with quantified uncertainty. Electric (E) field measurements were collected over 11 months from 12 sensors deployed in an urban environment. On the spatial scale, Polynomial Chaos Expansion (PCE) [1] combined with Bootstrap resampling [2] is used to model and predict exposure levels and spatial uncertainty. On the temporal scale, a Long Short-Term Memory (LSTM) [3] network is used for multi-step forecasting, and conformal prediction is employed to provide statistically valid confidence intervals. The proposed framework demonstrates improved reliability in exposure prediction and uncertainty estimation for continuous EMF monitoring in complex real-world environments.

1 Introduction

The rapid proliferation of wireless communication technologies, particularly with the deployment of 5G and beyond networks, has intensified public concern regarding radio frequency electromagnetic field (RF-EMF) exposure. Although guidelines and limits for EMF exposure have been established [4], continuous long-term monitoring is necessary to understand the trends and evolution of exposure levels. Measurement-based assessments are inherently affected by uncertainties arising from different sources, including device noise, spatial environmental variability, and temporal fluctuations in BS activity.
This work presents an RF-EMF exposure assessment framework that integrates spatial and temporal prediction based on Polynomial Chaos Expansion (PCE) and neural networks. Besides, different uncertainty quantification techniques are applied to spatial and temporal models. The proposed approach is evaluated using real-world data collected over 11 months from 12 sensors deployed in an urban environment, together with publicly available base station information, including antenna locations, orientations, and related parameters.

2 Problem statement

Let $x_s^t \in \mathcal{R}$ denote the exposure level at location $s \in \mathcal{S}$ and time $t \in \mathcal{T}$, $\mathcal{S}$ represents the set of sensor locations, and $\mathcal{T} = \{t_1, \ldots, t_T\}$ is the discrete set of temporal indices. Each sensor s is associated with auxiliary environmental information $\mathbf{c}(s)$. $x_{\mathcal{S}}^{\mathcal{T}}$ is used to represent the measured exposure levels across sensors and time. The objective of the exposure assessment framework is to estimate the exposure field across space and time based on historical measurements at known sensor sites and relevant environmental factors. Formally, the problem can be expressed as:

$$\hat{x}_s^{t+1} = \mathcal{M}(x_{\mathcal{S}}^{\mathcal{T}\leq t}, \mathbf{c}(s)) \tag{1}$$

where $\mathcal{M}$ denotes a surrogate model that emulates the spatiotemporal effects of the system on exposure, $\hat{x}_s^{t+1}$ indicates the estimation for x_s^{t+1}, and $\mathcal{T}\leq t$ denotes the set of all timestamps till t. The overall spatiotemporal prediction problem is decomposed into two independent modules: spatial module $\mathcal{M}_S$ and temporal module $\mathcal{M}^T$:

$$\mathcal{M}(x_S^{\mathcal{T}\leq t}, \mathbf{c}(s)) = \mathcal{M}_S(\mathbf{c}(s)) \odot \mathcal{M}^T(x_S^{\mathcal{T}\leq t}) \tag{2}$$

where $\odot$ indicates that the model consists of two components, rather than to imply a mathematical composition. The spatial $\mathcal{M}_S$ module is a mapping that takes environmental information as input and predicts exposure levels:

$$\mathcal{M}_S : \mathbf{c}(s) \rightarrow \hat{x}_s \tag{3}$$

A multi-step temporal forecasting module $\mathcal{M}^T$ forecasts the exposure given sensor's precedent observations:

$$\mathcal{M}^T : x^{\mathcal{T}\leq t} \rightarrow \hat{x}^{t+1:t+\tau} \tag{4}$$

where $\hat{x}^{t+1:t+\tau} = \{\hat{x}_{t+1}, \ldots, \hat{x}_{t+\tau}\}$, and τ is the number of steps to be predicted.

In the spatial part, PCE is employed for spatial prediction, which is a surrogate modeling technique that approximates a complex model as a weighted sum of orthogonal polynomial basis functions [1]. The temporal model is implemented using a three-layer LSTM network followed by a fully connected layer for forecasting.

For uncertainty quantification in the spatial model, it is performed using leave-one-out cross-validation (LOOCV) and bootstrap methods to capture data variability and assess model robustness. LOOCV is a model validation method which leaves one sample out for testing and rest for training. It is used to evaluate the model's generalization capability, and also allows quantifying the influence of individual observations on model stability. And bootstrap is a statistical technique for estimating uncertainty by generating multiple new datasets. Conformal prediction (CP) is adopted for uncertainty quantification with temporal model, which can provide reliable uncertainty estimates for any estimators. One basic assumption for CP is the exchangeability condition which requires that any reordering of the dataset is equiprobable. However, temporal data are inherently non-exchangeable due to their sequential dependencies. To address this, [5] proposes a conformal forecasting model which relaxed the exchangeability assumption and adopts CP for time series forecasting.

3 Experiments and results

The dataset is based on 12 sensors installed in Massy, where each sensor is activated every 2 hours to perform 6-min E-field measurement. In total, 4008 temporal samples are available from each sensor ranging from 2023-01-01 to 2023-12-01. Each sensor is associated with a unique ID. Figure 1 shows the installed sensors in red cross with marked sensor ID and their nearby base stations in green dots with antenna orientation in orange.

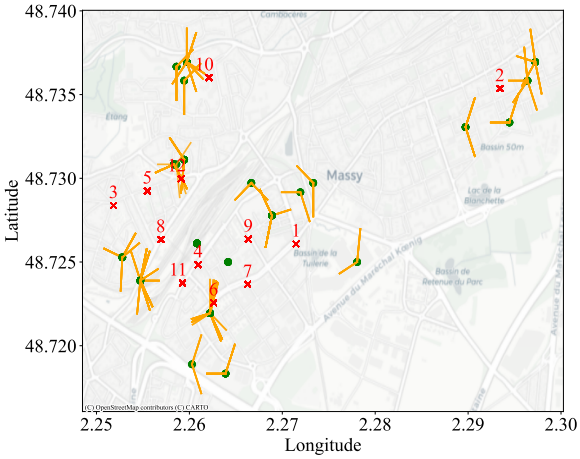

Figure 1: Sensors and BS locations in the urban environment

One day is divided into 12 2-hour blocks and the statistical distribution within each block is analyzed. To better visualize the temporal behavior of exposure levels, the measurements among three sensors (Sensor

4, 8 and 9) representing three levels of exposure are selected and presented in Figure 2. Despite differences in absolute levels between sensors, this general rising trend throughout the day appears to be a common pattern across the sensors. Most sensors exhibit slightly lower exposure levels during the early hours, followed by a gradual increase toward daytime and evening periods, where the field strength tends to stabilize or reach a mild peak. Notably, Sensor 4 records the highest exposure levels throughout the day, likely due to its proximity to a base station and the presence of multiple antennas oriented directly toward its location. The distribution on Sensor 9 appears bimodal, indicating the presence of two distinct exposure regimes. This suggests that the sensor may experience alternating levels of field strength, possibly due to varying network load, changes in antenna activity, or environmental factors.

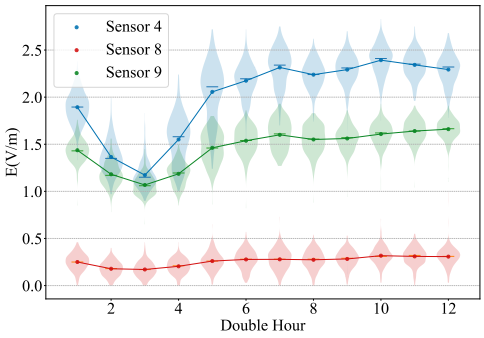

Figure 2: Distribution of two-hourly measurements. Marker dots, bar and shadowed area represent mean, median values and the distribution respectively

PCE was implemented for spatial exposure prediction. The performance of each model was evaluated using a LOO bootstrap strategy, which estimates prediction accuracy and model uncertainty for each sensor location. The box plot in Figure 3 compares predicted and true exposure levels for each sensor. Each box represents the variability in the bootstrap replications for a given sensor, capturing both the median and the interquartile range of predictions. The red stars denote the true observed values, while the percentage labels above each point indicate the relative deviation of the true value from the corresponding bootstrap mean.
Overall, the figure highlights notable heterogeneity across sensors, where some locations, such as Sensors 2 and 4, exhibit larger variability and deviations, suggesting higher model uncertainty or local environmental complexity. In contrast, other sensors (e.g., 3 and 9) show tight distributions and small Mean Absolute Percentage Error (MAPE), indicating more stable and reliable predictions at those sites. This spatial disparity reflects that some site-dependent parameters are not adequately represented in the current model. Consequently, model generalization appears to be sensitive to the local conditions.

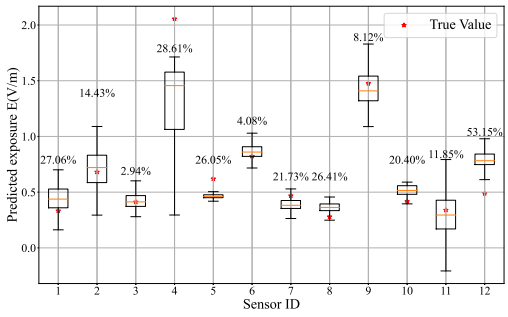

Figure 3: Bootstrapping with LOOCV for spatial exposure prediction

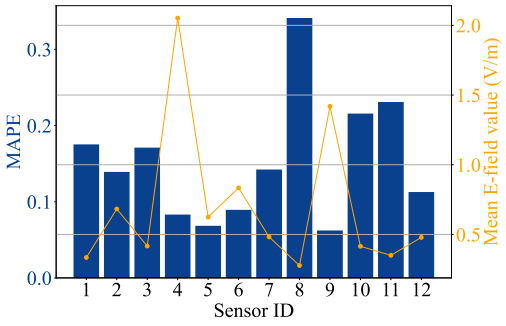

Figure 4: LSTM for temporal exposure forecasting

The temporal model consists of a three-layer LSTM network to predict future exposure levels based on historical observations. The data is partitioned into training, calibrating and testing sets with proportion of 70%, 10%, 20% respectively. Training was conducted using the Adam optimizer over 50 epochs with a batch size of 16, and Mean Squared Error (MSE) as training loss. Conformal intervals Γ_α then are calculated based on calibration set and trained model. Figure 4 illustrates the performance of the temporal model

with $L = 12$ and $\tau = 1$. It presents the MAPE for each sensor (blue bars) along with the corresponding mean exposure level (orange line). Most sensors exhibit moderate prediction errors, with MAPE values generally below 20%. The high MAPE on sensor 12 may be attributed to its low absolute exposure levels. When the denominator in percentage error is small, even minor absolute deviations in prediction can lead to a large relative error. Conversely, sensors with stronger E-field values (e.g., Sensors 4 and 9) tend to yield more stable predictions, although high variability in their measurements can still increase model uncertainty. This finding necessitates that quantifying this uncertainty is crucial for reliable RF exposure assessment, as it reflects the confidence in model predictions.

A temporal forecasting example is presented in Figure 5 with $L = 12$ and $\tau = 6$, on the sensor ID 4, 8 and 9. Each subplot shows the measured exposure sequence (blue line), the forecasted exposure (red dots), the target values (green dots) over time, with conformal intervals in orange for $\alpha = 0.1$. Overall, the results indicate that the LSTM model is able to capture the main temporal variations of the exposure level among sensors. The majority of the target values lie within the conformal intervals, demonstrating that the uncertainty quantification is well calibrated. Differences in conformal interval across sensors reflect varying levels of temporal variability and prediction difficulty, with more stable sensors exhibiting tighter intervals and more reliable forecasts.

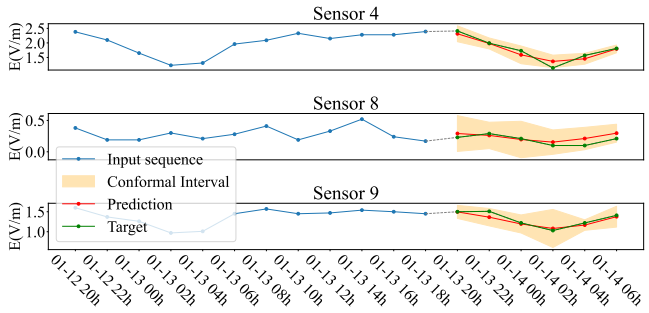

Figure 5: Temporal forecasting with prediction intervals

4 Conclusion

This study explores spatial and temporal prediction with uncertainty quantification by using measurement data from sensor networks. The sparse spatial data are modeled by introducing novel features that represent environmental information. Then PCE is adopted for spatial prediction and validated by using Bootstrap and LOOCV. The results show low MAPE error and low uncertainty at some sensors, and high MAPE on others. This heterogeneity may be caused by the heterogeneous environmental complexity. For the temporal model, the LSTM network is constructed, followed by CP to quantify the uncertainty. The overall forecasting performance is good, with most MAPE values below 20% and some even under 10%. The further step is to integrate spatial prediction with temporal forecasting to achieve spatio-temporal prediction for more comprehensive uncertainty assessment. Besides, incorporating uncertainty-aware exposure assessments into operational Radio Resource Management strategies is worth exploration, which offers a pathway for proactive network optimization. By anticipating fluctuations in EMF levels, the system can implement preemptive measures—such as dynamic power tuning or intelligent load balancing—to minimize environmental impact during peak periods without compromising service reliability

References

[1] Stefano Marelli and Bruno Sudret. “UQLab: A framework for uncertainty quantification in Matlab”. In: *Vulnerability, uncertainty, and risk: quantification, mitigation, and management*. 2014, pp. 2554–2563.

[2] Bradley Efron. “Bootstrap Methods: Another Look at the Jackknife”. In: *The Annals of Statistics* 7.1 (1979), pp. 1–26.

[3] Sepp Hochreiter and Jürgen Schmidhuber. “Long short-term memory”. In: *Neural computation* 9.8 (1997), pp. 1735–1780.

[4] ICNIRP. “Guidelines for limiting exposure to electromagnetic fields (100 KHz to 300 GHz)”. In: *Health physics* 118 (5 2020), pp. 483–524.

[5] Kamile Stankeviciute, Ahmed M Alaa, and Mihaela Van der Schaar. “Conformal time-series forecasting”. In: *Advances in neural information processing systems* 34 (2021), pp. 6216–6228.